High-Resolution Imaging Satellite Constellation*

Xiaohua Li[1], Lhamo Dorje[1], Yezhan Wang[1], Yu Chen[1], and Erika Ardiles-Cruz[2]

[1] Binghamton University, Binghamton NY 13902, USA
[2] The U.S. Air Force Research Laboratory, Rome, NY 13441, USA
{xli,ldorje1,ywang516,ychen}@binghamton.edu, erika.ardiles-cruz@us.af.mil

Abstract. Large-scale Low-Earth Orbit (LEO) satellite constellations have wide applications in communications, surveillance, and remote sensing. Along with the success of the SpaceX Starlink system, multiple LEO satellite constellations have been planned and satellite communications has been considered a major component of the future sixth generation (6G) mobile communication systems. This paper presents a novel LEO satellite constellation imaging (LEOSCI) concept that the large number of satellites can be exploited to realize super high-resolution imaging of ground objects. Resolution of conventional satellite imaging is largely limited to around one meter. In contrast, the LEOSCI method can achieve imaging resolution well below a centimeter. We first present the new imaging principle and show that it should be augmented with a Dynamic Data Driven Applications Systems (DDDAS) design. Then, based on the practical Starlink satellite orbital and signal data, we conduct extensive simulations to demonstrate a high imaging resolution below one centimeter.

Keywords: THz imaging · LEO satellite constellation · Synthetic aperture radar (SAR) · Integrated communication and sensing · Starlink.

1 Introduction

Spaceborne imaging systems have wide applications, including surveillance and remote sensing [11]. Typically, satellite-based sensing can use a synthetic aperture, e.g., for radar (SAR), to generate ground images, but the resolution is relatively low. The state of the art of the current satellite SAR imaging resolution is around one meter. Increasing resolution has always been a highly-demanded, but challenging objective of satellite-based imaging.

Along with the development of SpaceX's Starlink satellite constellation, which has over 2000 satellites deployed in space and over $50,000$ satellites planned to deploy, it has become a promising research topic to use LEO satellite constellations for global communications, including WiFi wireless access and the future sixth generation (6G) mobile communications [5]. Several large-scale LEO

* Thanks to Erik Blasch and Alex Aved for concept development and co-authorship. This work is supported by the U.S. Air Force Office of Scientific Research (AFOSR) under Grant FA9550-20-1-0237.

(a) (b)

Fig. 1. (a) Conventional single-satellite SAR imaging. (b) Proposed LEO satellite constellation imaging (LEOSCI) with high resolutions to sense small targets.

satellite constellations are deployed or in planning. They are designed mainly for communications because only the large mobile communications market can cover the huge cost of their deployment and maintenance. Reusing them as a sensing and imaging platform via the integrated communication and sensing design [9] is both interesting and attractive since it will create novel applications and generate new revenues.

This paper develops a novel LEO satellite constellation imaging (LEOSCI) method that uses a large number of satellites to create ground target images with a super-high resolution well below one centimeter. By comparison, as the state-of-the-art of existing commercial satellite imaging, optical camera imaging resolution is 0.3 meters and SAR imaging resolution is much lower, around one meter. To guarantee the performance of this complex imaging system in a dynamic environment, Dynamic Data Driven Applications Systems (DDDAS) design principles [3] will be adopted to address the challenging multi-objective parameterization among imaging resolution, imaging area, number of satellites, imaging time delay, multiple satellite data collection, and data processing. We will use the realistic data of the SpaceX Starlink to conduct simulations to demonstrate the effectiveness of the LEOSCI method.

The organization of this paper is as follows. Section 2 describes the LEO satellite constellation imaging model. Section 3 develops the imaging algorithm and Section 4 presents simulation results. Conclusions are given in Section 5.

2 Model of Satellite Constellation Imaging

Large-scale LEO satellite constellations such as Starlink create a cellular structure similar to mobile networks, with satellite antenna beams replacing terrestrial cellular towers [14]. At any given time, a cell on the ground is illuminated by one or more beams. The size of the cell is determined by the beam width. Each satellite beam only serves this cell for a short time. The cell is continuously served by the satellites flying over.

Existing works that use satellites for ground imaging [6][10] in general apply the synthetic aperture method from only one satellite, as shown in Fig. 1(a).

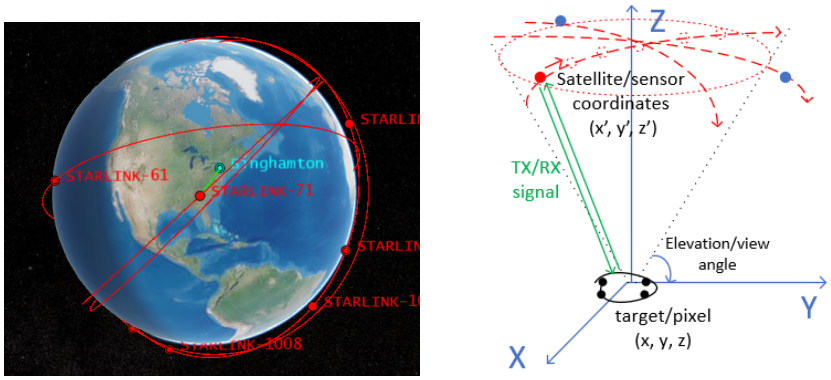

(a) (b)

Fig. 2. (a) Orbits of some Starlink satellites and the illumination of the target Binghamton by satellite STARLINK-71 (green line). (b) Coordinates of satellites and target. A satellite (red dot) enters the sensing area (red dotted circle) of the target and starts collecting sensing data at various locations along its orbit.

The Y-direction (range) resolution is $\Delta Y = \frac{c}{2B}$, where c is the speed of light and B is the signal bandwidth. Starlink has beam signal bandwidth 250 MHz, so the ground resolution will be 0.85 meters (assuming a 45° incidence angle).

For high-resolution imaging, we propose to use many satellites instead of one only and use imaging techniques developed in millimeter-wave/Tera-Hz (THz) imaging such as airport screening systems [2] [4]. As shown in Fig. 1(b), in an LEO satellite constellation, many satellites will fly over the imaging area sequentially. We call them *valid* satellites. When a valid satellite flies over the area, it keeps illuminating the target and recording the reflected echos. Either a communication signal or radar signal can be sent. Multiple satellites within this area can transmit and receive at the same time, just with different frequencies. These satellites' data will be collected and processed together to generate an image of the target. The satellites effectively form a virtual antenna array. The size of this array is the synthetic aperture and determines the imaging resolution.

This LEO satellite constellation imaging concept is a new opportunity with a lot of challenges. One of the major challenges is that only a small number of satellites within the constellation can sense a target, which can hardly form a dense and regular array. THz imaging requires a dense 2D antenna array with antennas evenly spaced at a half-wavelength distance. For example, an array used 736 transmit (Tx) antennas and 736 receive (Rx) antennas to electronically scan 25,600 antenna positions within a regular grid of 50cm×50cm aperture [1]. This kind of scan over a 2D regular grid is impossible for satellites. To address this challenge, we adopt the algorithm developed in [8] and will show by simulations that a few satellites are indeed enough.

3 Imaging Algorithm and Resolution

Consider the case that a satellite flies over the target area, transmits a sensing signal, and collects the target echos. As an illustration, Fig. 2(a) shows the STARLINK-71 satellite moves along its orbit and passes over the target located in Binghamton, NY. It keeps sensing the target until flying out of the sensing area, as illustrated in Fig. 2(b). The sensing area is determined by the elevation or viewing angle of the target, which further determines the number of valid satellites and imaging delay.

Assume the coordinates of the satellite and the target are $\mathbf{r}' = (x', y', z')$ and $\mathbf{r} = (x, y, z)$, respectively. The satellite transmits signal $p(t)$ with carrier frequency f_c, and receives the signal $\hat{s}_{\mathbf{r}'}(t)$ reflected by the target,

$$\hat{s}_{\mathbf{r}'}(t) = \int_{\mathbf{r}} \sigma_{\mathbf{r}} p(t - \tau_{\mathbf{r}'\mathbf{r}}) d\mathbf{r} + \hat{v}_{\mathbf{r}'}(t), \tag{1}$$

where $\tau_{\mathbf{r}'\mathbf{r}}$ is the propagation delay, $\sigma_{\mathbf{r}}$ is the target's reflection coefficient, and $\hat{v}_{\mathbf{r}'}(t)$ denotes noise, interference, and clutter [13]. The satellite can transmit either Frequency-Modulated Continuous Wave (FMCW) radar signal waveform [6] or communications signal such as Digital Video Broadcasting - Satellite - 2nd Generation (DVB-S2X) signal waveform [12]. Conventional pulsed radar signals may not be appropriate due to the limited peak transmission power of the communication satellites. Using communication signals directly for sensing is more attractive as it reduces hardware complexity and cost.

With the signal processing outlined in [8], we get a data sample at each sensing position $\mathbf{r}'$ which is

$$s_{\mathbf{r}'} = \int_{\mathbf{r}} \sigma_{\mathbf{r}} e^{j2\pi f_c \tau_{\mathbf{r}'\mathbf{r}}} d\mathbf{r} + v_{\mathbf{r}'}, \tag{2}$$

where $v_{\mathbf{r}'}$ denotes the processed $\hat{v}_{\mathbf{r}'}(t)$. For 2D imaging, the goal is to reconstruct an $I \times J$ target image $\mathbf{X}$ whose pixel is X_{ij}. We stack the columns of $\mathbf{X}$ into an N-dimensional column vector $\mathbf{x} = \text{vec}(\mathbf{X})$, where $N = IJ$. Assume we have collected M data samples from M satellite sensing positions $\mathbf{r}'_m = (x'_m, y'_m, z'_m)$, $m = 0, \cdots, M-1$. We stack the data into an M-dimensional column vector $\mathbf{y}$, whose mth element is $y_m = s_{\mathbf{r}'_m}$. Then we have

$$\mathbf{y} = \mathbf{H}\mathbf{x} + \mathbf{v}, \tag{3}$$

where the element of the $M \times N$ matrix $\mathbf{H}$ is $H_{mn} = e^{j4\pi R_{mn}/\lambda}$, R_{mn} is the distance between the satellite and the target, and λ is the wavelength. The vector $\mathbf{v}$ includes noise, interference, and clutter.

Based on Eq.(3), one can apply the computationally efficient back-projection (BP) algorithm to reconstruct the image, which gives

$$\hat{\mathbf{x}} = \mathbf{H}^H \mathbf{y}. \tag{4}$$

where $(\cdot)^H$ is the Hermitian transpose. The computational complexity is $O(MN)$. From Eqs.(3) and (4), one can easily see that an extremely large number of antenna samples, i.e., large M, is needed to make $\mathbf{H}^H\mathbf{H}$ close to the identity. This

is why a large-scale LEO satellite constellation is needed. Fortunately, each satellite is able to collect a large number of data samples along its orbit. So the BP may just need a few valid satellites for each sensing area.

The signal-to-noise ratio (SNR) of the received signal can be derived as

$$\text{SNR} = \frac{P_t G_t G_r \lambda^2 \theta \Delta_S \sigma_0}{(4\pi R)^3 k T B F L_s}. \tag{5}$$

where P_t is the transmit power, G_r is the receive antenna gain, G_t is the transmit antenna gain, θ is the beam width, Δ_S is the resolution, σ_0 is the radar cross section (RCS) of the target, R is the range, and L_s is the system loss. The noise power is $P_N = kTBF$ where T is the noise temperature, k is the Boltzmann constant, B is the signal bandwidth, and F is the noise factor of the system.

The imaging resolution is

$$\Delta X = \Delta Y = \frac{\lambda R}{2D} \tag{6}$$

where D is the array aperture in each dimension [13]. D is determined by the satellite height and the target elevation angle.

The imaging resolution and quality depend on a lot of factors in a complex way. Smaller elevation angle leads to more valid satellites, larger D, and better resolution, but suffers from longer imaging delay, lower SNR, etc. It is computationally complex to generate a high-resolution image over a large area. It is challenging to guarantee the performance of high resolution imaging in dynamic environments with uncertain propagation attenuation and target reflectivity. Following the DDDAS design principle, we can apply the dynamic feedback control to achieve desired trade-offs [3]. Specifically, starting from a coarse image of a large area, DDDAS leverages continuous sensor measurement data and imaging model to adaptively adjust satellite configuration, signal power/beam width, and image pixel size. This way, we can generate finer images over smaller areas with an affordable complexity [8][15]. Applying the DDDAS concept in the development of this complex system, the super-high resolution images obtained in real-time will enable an application to dynamically incorporate new information to make the working procedure be more adaptive to the environment accurately.

4 Simulation Results

We compared the proposed LEOSCI method with the conventional single-satellite SAR imaging based on the practical SpaceX Starlink satellite constellation data. Specifically, we used the Starlink's two-line element (TLE) file [3] to get the orbital information and coordinates of all the satellites. The July 7, 2022 TLE file consisted of 2469 Starlink satellites. We simulated a target located at the coordinates of Binghamton, NY. With an elevation angle of 30°, we had 435 valid satellites. All the satellites are shown in Fig. 3. Their distance to the target was around

[3] Downloaded from https://celestrak.org/

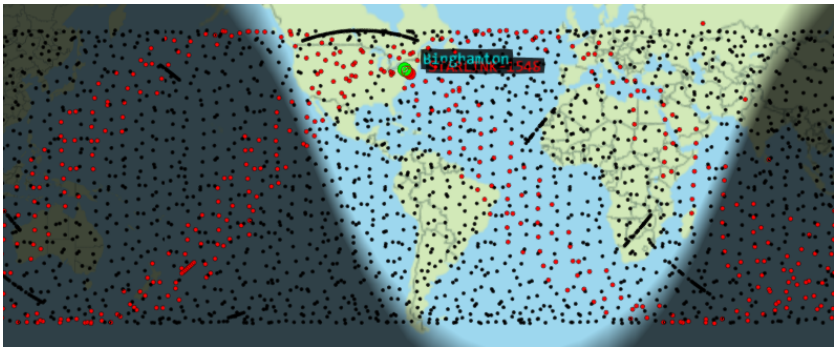

Fig. 3. Starlink satellite constellation on July 7 2022 13:41:11. Satellites are shown as black and red dots. Red dots are the valid satellites that can contribute to imaging the target located at Binghamton, NY (green dot). At this moment, two satellites (bigger red dots) can sense the target.

$R = 462$ km. This means we had an effective radar aperture of 1600×1600 km^2, i.e. $D = 1600$ km. The theoretical resolution is thus $\Delta X = \Delta Y = 0.004$ meter according (6).

We applied the typical Starlink signal parameters [14]: Carrier frequency $f_c = 11.7$ GHz, bandwidth $B = 250$ MHz, beam width 2.5°, antenna gain $G_t = G_r = 53$ dB, noise power $P_N = -120$ dB, system loss $L_s = 6$ dB, transmit power $P_t = 37$ dBW. If the signal dechirping or cross-correlation provides 30 dB gain, then we have 19 dB SNR for target RCS $\sigma_0 = 100$ and 1 centimeter resolution.

To generate the simulation data, we created a target consisting of two circles as shown in Fig. 4(a): 4 points on the inner circle of radius 0.02 meter and 8 points on the outer circle of radius 0.05 meter. We simulated the satellite signal waveforms as either FMCW radar wave or DVB-S2X wave. Each of the valid satellites conducted a transmission and receiving at each of the 435 randomly selected locations on its orbit. The received signals were dechirped in the case of FMCW or cross-correlated with the transmitted signal in the case of DVB-S2X to find the maximum samples, which resulted in a 435×435 data matrix. So $M = 189225$. With the data matrices, we reconstructed images with size $I \times J = 30 \times 30$ (so $N = 900$) for the target area of 0.1×0.1 meter^2 based on (4).

Figures 4(b) and (c) show the reconstructed images with the LEOSCI method when the satellite signal was FMCW and DVB-S2X waveforms, respectively. For comparison, Fig. 4(d) shows the reconstructed image with the conventional single-satellite SAR method. Image reconstruction quality was compared quantitatively in Table 1 in terms of peak-signal-to-noise ratio (PSNR), structural similarity method (SSIM) [7], and mean square error (MSE) between the reconstructed image and the true image of Fig. 4(a).

It is easy to see that the LEOSCI method could provide a super high imaging resolution of less than 1 centimeter, while the conventional SAR failed completely due to insufficient resolution. The true image shown in Fig. 4(a) had a larger size

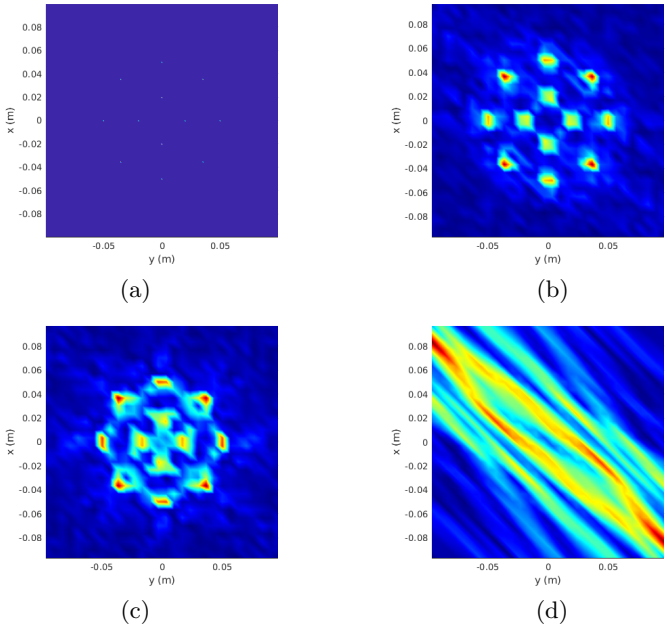

Fig. 4. (a) True target. (b) Target image reconstructed by the LEOSCI method with FMCW waveform. (c) Target image reconstructed by the LEOSCI method with DVB-S2X waveform. (d) Target image reconstructed by conventional single-satellite SAR.

of 200×200 pixels. It was resized to 30×30 pixels when calculating performance metrics. The reconstructed images in Figs. 4(b) and (c) in fact looked much more similar to the resized true image than to Fig. 4(a).

Table 1. Comparison of imaging quality and (theoretical) imaging resolution.

Imaging Method	Resolution (m)	PSNR (dB)	SSIM	MSE
LEOSCI (FMCW)	0.004	15.0818	0.0697	0.0310
LEOSCI (DVB-S2X)	0.004	16.3638	0.0840	0.0231
Single-Satellite SAR	0.85	8.6805	0.0081	0.1355

5 Conclusions

It has been well recognized to leverage the large number of satellites for global communications, but there is not sufficient attention given to their capability as a sensing and imaging constellation. The satellite constellation is potential to serve the compelling need of DDDAS in the space applications. This paper proposes the LEO satellite constellation imaging (LEOSCI) concept that exploits a few set of valid satellites to generate super high-resolution images. Simulations

demonstrate that the method can provide ground target images with resolution lower than one centimeter, which is hardly achievable by existing satellite SAR imaging. As future work, we will verify the imaging algorithm with real-measured millimeter wave radar data and verify the LEOSCI concept using UAVs (unmanned aerial vehicles) to collect data.

References

1. Ahmed, S.S., Schiessl, A., Schmidt, L.P.: A novel fully electronic active real-time imager based on a planar multistatic sparse array. IEEE Transactions on Microwave Theory and Techniques **59**(12), 3567–3576 (2011)
2. Alexander, N.E., Alderman, B., Allona, F., Frijlink, P., Gonzalo, R., Hägelen, M., Ibáñez, A., Krozer, V., Langford, M.L., Limiti, E., et al.: Terascreen: Multi-frequency multi-mode terahertz screening for border checks. In: Passive and Active Millimeter-Wave Imaging XVII. vol. 9078, p. 907802. International Society for Optics and Photonics (2014)
3. Blasch, E., Ravela, S., Aved, A.: Handbook of dynamic data driven applications systems. Springer (2018)
4. Cooper, K.B., Dengler, R.J., Llombart, N., Thomas, B., Chattopadhyay, G., Siegel, P.H.: Thz imaging radar for standoff personnel screening. IEEE Transactions on Terahertz Science and Technology **1**(1), 169–182 (2011)
5. Giordani, M., Zorzi, M.: Non-terrestrial networks in the 6g era: Challenges and opportunities. IEEE Network **35**(2), 244–251 (2020)
6. Hoogeboom, P., Hanssen, R., Pastena, M., Imbembo, E., van Duijn, P., Otten, M., Monni, S., Hoogeboom, P., Hanssen, R., Pastena, M., et al.: Panelsar, an fmcw based x-band smallsat sar for infrastructure monitoring. In: The 27th Annual AIAA/USU Conference on Small Satellites, Logan, USA. pp. 1–5 (2013)
7. Hore, A., Ziou, D.: Image quality metrics: Psnr vs. ssim. In: 2010 20th international conference on pattern recognition. pp. 2366–2369. IEEE (2010)
8. Li, X., Chen, Y.: Lightweight 2d imaging for integrated imaging and communication applications. IEEE Signal Processing Letters **28**, 528–532 (2021)
9. Liu, F., Cui, Y., Masouros, C., Xu, J., Han, T.X., Eldar, Y.C., Buzzi, S.: Integrated sensing and communications: Towards dual-functional wireless networks for 6g and beyond. IEEE journal on selected areas in communications (2022)
10. Liu, Y., Deng, Y.K., Wang, R., Loffeld, O.: Bistatic fmcw sar signal model and imaging approach. IEEE Transactions on Aerospace and Electronic Systems **49**(3), 2017–2028 (2013)
11. Majumder, U.K., Blasch, E.P., Garren, D.A.: Deep Learning for Radar and Communications Automatic Target Recognition. Artech House (2020)
12. Pisciottano, I., Santi, F., Pastina, D., Cristallini, D.: Dvb-s based passive polarimetric isar—methods and experimental validation. IEEE Sensors Journal **21**(5), 6056–6070 (2020)
13. Richards, M.A., Scheer, J., Holm, W.A., Melvin, W.L.: Principles of modern radar. Citeseer (2010)
14. Sayin, A., Cherniakov, M., Antoniou, M.: Passive radar using starlink transmissions: A theoretical study. In: 2019 20th International Radar Symposium (IRS). pp. 1–7. IEEE (2019)
15. Wu, R., Liu, B., Chen, Y., Blasch, E., Ling, H., Chen, G.: A container-based elastic cloud architecture for pseudo real-time exploitation of wide area motion imagery (wami) stream. Journal of Signal Processing Systems **88**(2), 219–231 (2017)